

Electronic Supplementary Information

Oxygen-powered sustainable FePO₄ preparation for sodium metal batteries with Li acetate recovery

Fumiyasu Nozaki¹, Shaoning Zhang¹, Jinkwang Hwang^{1,*}, Martin Hoffmann Petersen², Jin Hyun Chang², Juan María García-Lastra², and Kazuhiko Matsumoto^{1,*}

¹Graduate School of Energy Science, Kyoto University, Yoshida-honmachi, Sakyo-ku, Kyoto 606-8501, Japan.

²Department of Energy Conversion and Storage, Technical University of Denmark, 2800 Kgs. Lyngby, Denmark

Corresponding Author

*E-mail: hwang.jinkwang.5c@kyoto-u.ac.jp

*E-mail: matsumoto.kazuhiko.4c@kyoto-u.ac.jp

Keywords: Sodium metal batteries, FePO₄, olivine, triphylite, sustainable delithiation

Electrochemical test procedures of the pristine and R-LFP

The LiFePO₄ positive electrodes were prepared by mixing the pristine or R-LFP with Super C65 carbon black (MTI) and polyvinylidene fluoride (PVDF, Kureha) (80:15:5 wt%) in *N*-methyl-2-pyrrolidone (NMP, Fujifilm Wako Pure Chemicals, purity of >99.0%) using a planetary mixer (AR-100, Thinky). The mixture was thereafter pasted onto Al foil and dried at 60 °C for 3 h. The dried electrode was punched into discs (diameter: 10 mm) and then vacuum-dried overnight at 80 °C. Under a dry Ar atmosphere (H₂O < 1 ppm and O₂ < 1 ppm) in a glove box, 2032-type coin cells were assembled. The lithium metal (Sigma-Aldrich, purity of 99.9%) that was cut into a disk (diameter of 13 mm) and attached to a stainless-steel plate current collector was used as a negative electrode. As the electrolyte, 1 mol dm⁻³ Li[PF₆]-EC/DMC (1:1 v/v) (Kishida chemical) was selected. A glass fiber (Whatman GF/A) was used as a separator. Charge–discharge properties were tested using a charge-discharge test device (HJ1001SD8, Hokuto Denko) at 25 °C. The cutoff voltage and C-rate were set in the 2.0–4.2 V range and 0.05C (1C = 170 mA g⁻¹), respectively. The capacity was calculated based on the weight of the LiFePO₄ active material.

Table S1 Crystallographic data of the P-LFP by the Rietveld refinement.

LiFePO ₄ (Space group: <i>Pnma</i>)						
$R_p = 16.0\%$, $R_{wp} = 11.5\%$						
<hr/>						
	a (Å)	b (Å)	c (Å)	V (Å ³)		
<hr/>						
	10.32279(8)	6.00338(4)	4.68896(4)	290.582(4)		
<hr/>						
Atom	Wyckoff symbol	x	y	z	B (Å ²)	Occ.
<hr/>						
Li	4 <i>a</i>	0	0	0	0.5	1.000
Fe	4 <i>c</i>	0.28229(9)	0.2500	0.9759(3)	0.5	1.000
P	4 <i>c</i>	0.0958(2)	0.2500	0.4227(5)	0.5	1.000
O1	4 <i>c</i>	0.0967(5)	0.2500	0.7423(8)	0.5	1.000
O2	4 <i>c</i>	0.4560(6)	0.2500	0.2088(7)	0.5	1.000
O3	8 <i>d</i>	0.1654(3)	0.0476(5)	0.2853(5)	0.5	1.000

The starting parameters were taken from a previous report¹, and the B factor and Occupancy were fixed at 0.5 and 1.0, respectively.

Table S2 Crystallographic data of the PO-FP by the Rietveld refinement.

FePO ₄ (Space group: <i>Pnma</i>)						
$R_p = 14.9\%$, $R_{wp} = 9.9\%$						
<hr/>						
	a (Å)	b (Å)	c (Å)	V (Å ³)		
<hr/>						
	9.81209(12)	5.78685(6)	4.78223(6)	271.540(5)		
<hr/>						
Atom	Wyckoff symbol	x	y	Z	B (Å ²)	Occ.
<hr/>						
Fe	4 <i>c</i>	0.27329(10)	0.2500	0.9498(2)	0.5	1.000
P	4 <i>c</i>	0.09449(18)	0.2500	0.4010(4)	0.5	1.000
O1	4 <i>c</i>	0.1222(3)	0.2500	0.7028(8)	0.5	1.000
O2	4 <i>c</i>	0.4410(4)	0.2500	0.1619(6)	0.5	1.000
O3	8 <i>d</i>	0.1705(3)	0.0413(4)	0.2552(4)	0.5	1.000

The starting parameters were taken from a previous report¹, and the B factor and Occupancy were fixed at 0.5 and 1.0, respectively.

Table S3 Organic elemental analysis of the recovered lithium acetate.

Element	Composition (wt%)
H	5.0
C	33.9

Table S4 Crystallographic data of the R-LFP by the Rietveld refinement.

LiFePO ₄ (Space group: <i>Pnma</i>)						
$R_p = 12.1\%$, $R_{wp} = 8.3\%$						
<hr/>						
	a (Å)	b (Å)	c (Å)	V (Å ³)		
	10.3146(3)	6.00458(14)	4.69769(13)	290.952(13)		
<hr/>						
Atom	Wyckoff symbol	x	y	z	B (Å ²)	Occ.
<hr/>						
Li	$4a$	0	0	0	0.5	1.000
Fe	$4c$	0.28317(11)	0.2500	0.9736(4)	0.5	1.000
P	$4c$	0.0977(3)	0.2500	0.4199(6)	0.5	1.000
O1	$4c$	0.1025(6)	0.2500	0.7297(10)	0.5	1.000
O2	$4c$	0.4599(7)	0.2500	0.2089(9)	0.5	1.000
O3	$8d$	0.1595(4)	0.0472(7)	0.2750(6)	0.5	1.000

The starting parameters were taken from a previous report¹, and the B factor and Occupancy were fixed at 0.5 and 1.0, respectively.

Table S5 Crystallographic data of RO-FP by the Rietveld refinement.

FePO ₄ (Space group: <i>Pnma</i>)						
$R_p = 16.3\%$, $R_{wp} = 10.6\%$						
<hr/>						
	a (Å)	b (Å)	c (Å)	V (Å ³)		
<hr/>						
	9.8196(3)	5.79774(17)	4.77120(17)	271.632(16)		
<hr/>						
Atom	Wyckoff symbol	x	y	z	B (Å ²)	Occ.
<hr/>						
Fe	4 <i>c</i>	0.27397(18)	0.2500	0.9511(4)	0.5	1.000
P	4 <i>c</i>	0.0940(3)	0.2500	0.3908(7)	0.5	1.000
O1	4 <i>c</i>	0.1309(6)	0.2500	0.6895(14)	0.5	1.000
O2	4 <i>c</i>	0.4501(8)	0.2500	0.1436(11)	0.5	1.000
O3	8 <i>d</i>	0.1734(5)	0.0549(7)	0.2453(7)	0.5	1.000

The starting parameters were taken from a previous report¹, and the B factor and Occupancy were fixed at 0.5 and 1.0, respectively.

Table S6 Comparison of the capacity, average voltage, and energy density calculated based on the total mass of positive and negative active materials in this study and several phosphate full cell systems²⁻⁵.

Full cell system	N/P ratio	Capacity (mAh g ⁻¹)	Average voltage (V)	Energy density (Wh kg ⁻¹)	Temperature (°C)	Rate or current density	Reference
Na/FePO ₄	1.20	128	2.86	364	90	10 mA (g-FePO ₄) ⁻¹	This work
Na/FePO ₄	0.56	108	2.78	300	25	10 mA (g-FePO ₄) ⁻¹	This work
O-CCF/Na ₃ V ₂ (PO ₄) ₃	0	74.3	3.4	252	Room temp.	1 mA cm ⁻²	2
Na/Na ₃ V ₂ (PO ₄) ₃	1.97	83.8	3.34	268	25	0.2C	3
Na/Na ₃ V ₂ (PO ₄) ₃	1.81	80.6	3.34	280	90	0.2C	3
Na/Na ₃ V ₂ (PO ₄) ₂ F ₃	4	83.4	3.54	295	25	1C	4
Graphite-Na/Na ₄ Fe ₃ (PO ₄) ₂ (P ₂ O ₇)	-	81.7	3.0	245	25	0.75 mA cm ⁻²	5

Table S7 Comparison of the capacity, average voltage, and energy density calculated based on the total mass of positive and negative active materials in this study.

FePO₄ source	FePO₄ mass loading (mg cm⁻²)	N/P ratio	Capacity (mAh g⁻¹)	Average voltage (V)	Energy density (Wh kg⁻¹)	Temperature (°C)	Rate (mA (g-FePO₄)⁻¹)
PO-FP	9.9	1.20	128	2.85	364	90	10
RO-FP	8.4	0.56	108	2.78	300	25	10
RO-FP	8.4	0.56	94	2.65	248	25	100
RO-FP	8.1	1.44	97	2.79	270	25	10
RO-FP	8.1	1.44	80	2.65	213	25	100

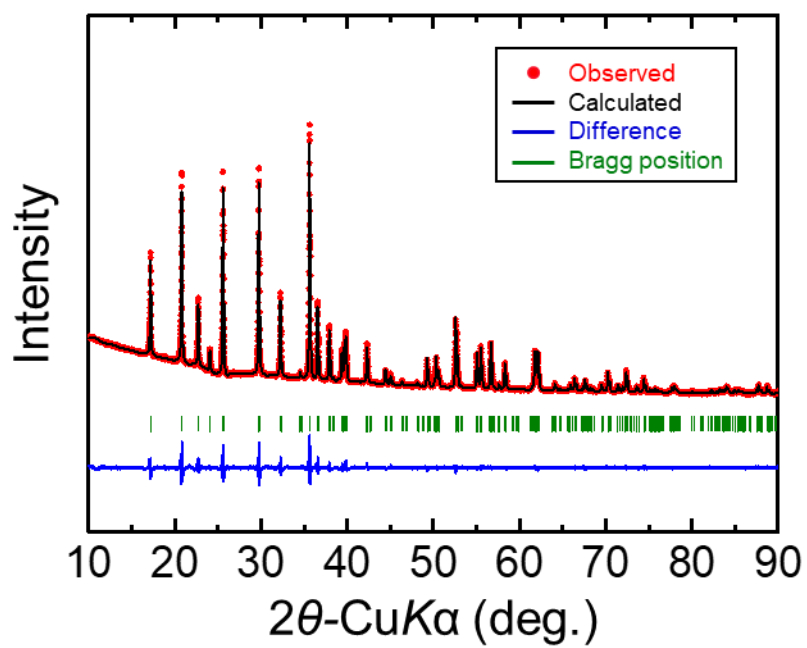


Fig. S1 Rietveld refinement result of the P-LFP.

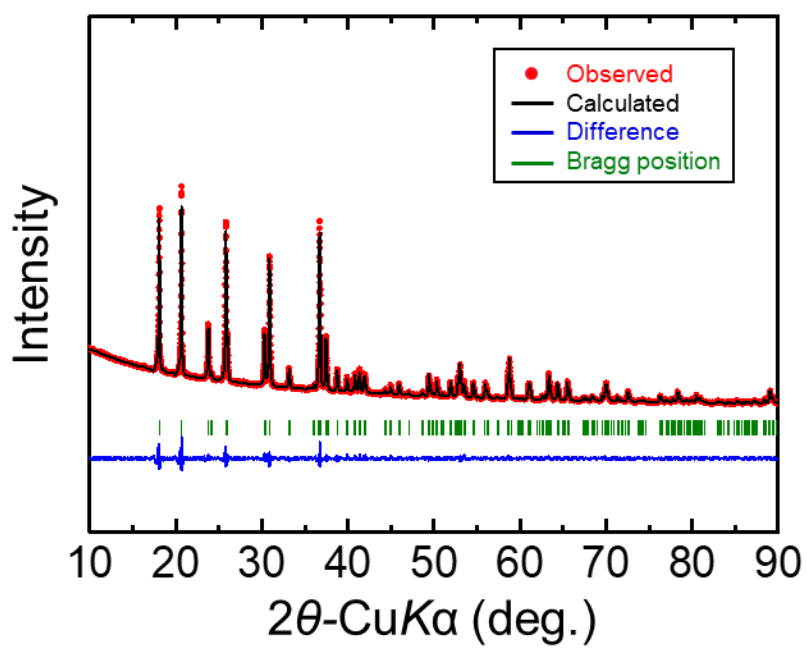


Fig. S2 Rietveld refinement result of the PO-FP.

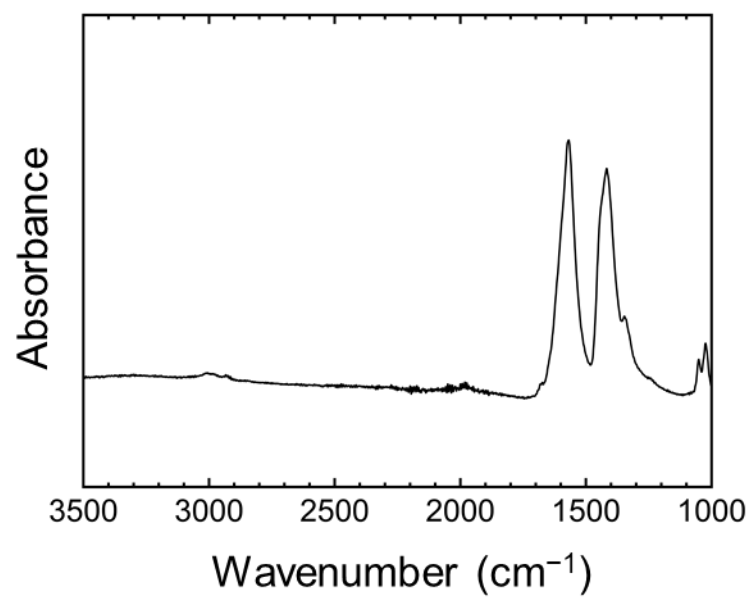


Fig. S3 FT-IR spectra of the recovered lithium acetate.

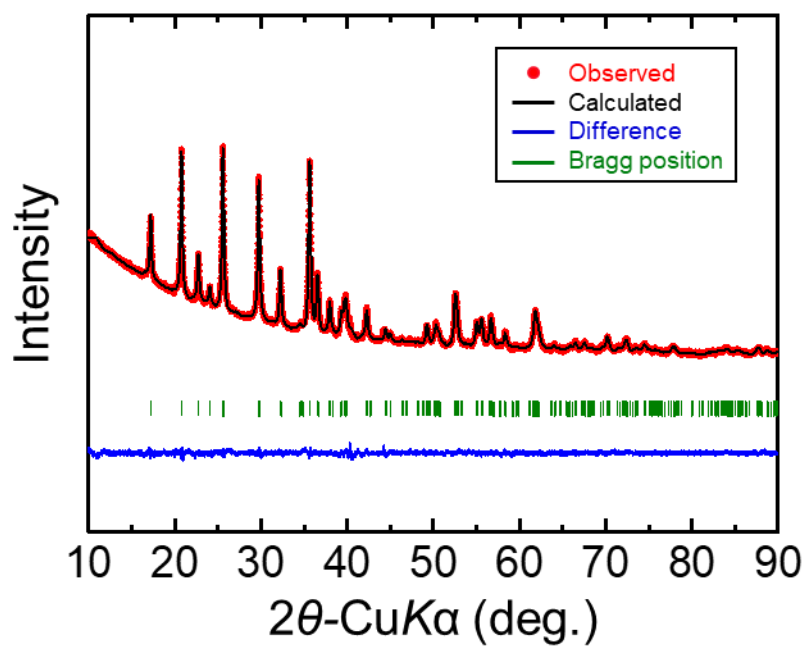


Fig. S4 Rietveld refinement result of the R-LFP.

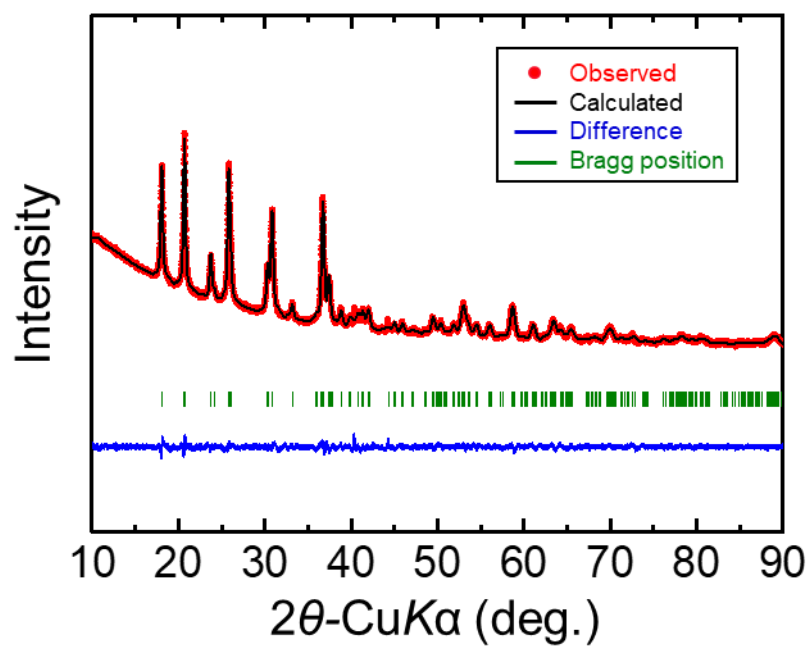


Fig. S5 Rietveld refinement result of the RO-FP.

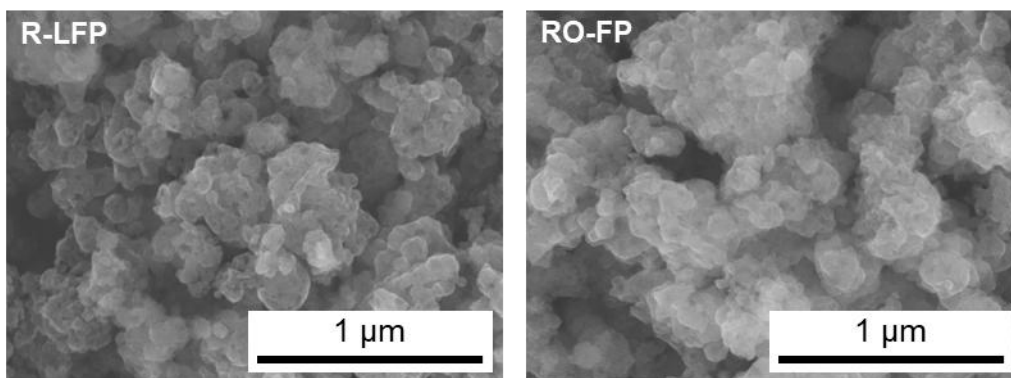


Fig. S6 SEM images of R-LFP and RO-FP.

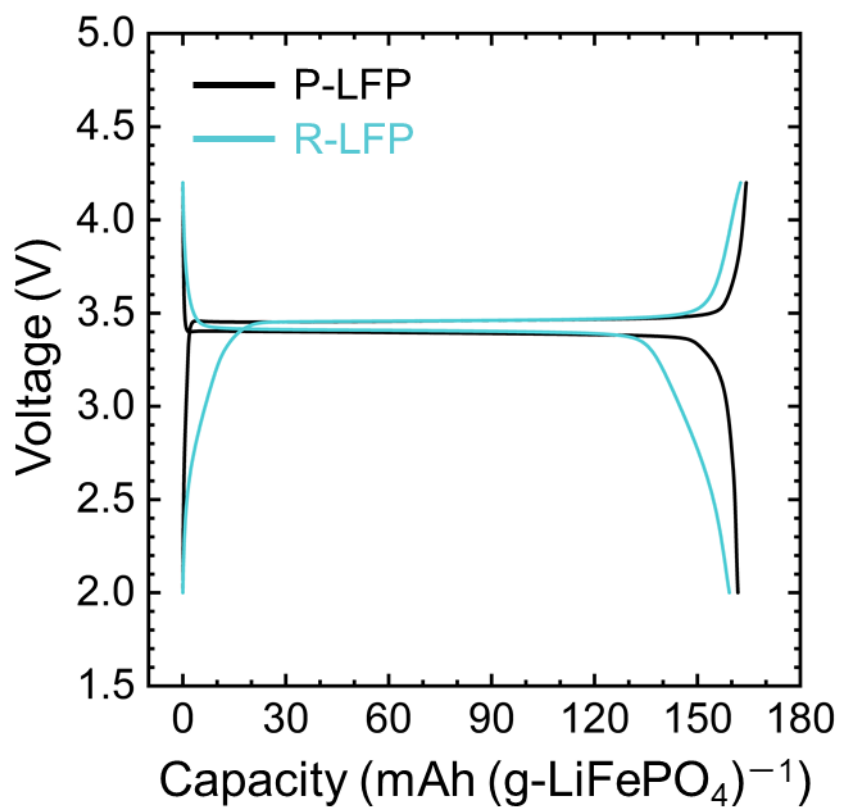


Fig. S7 Charge–discharge curves of the Li/P-LFP and Li/R-LFP half cells at 25 °C. C-rate: 0.05C (1C = 170 mA g⁻¹).

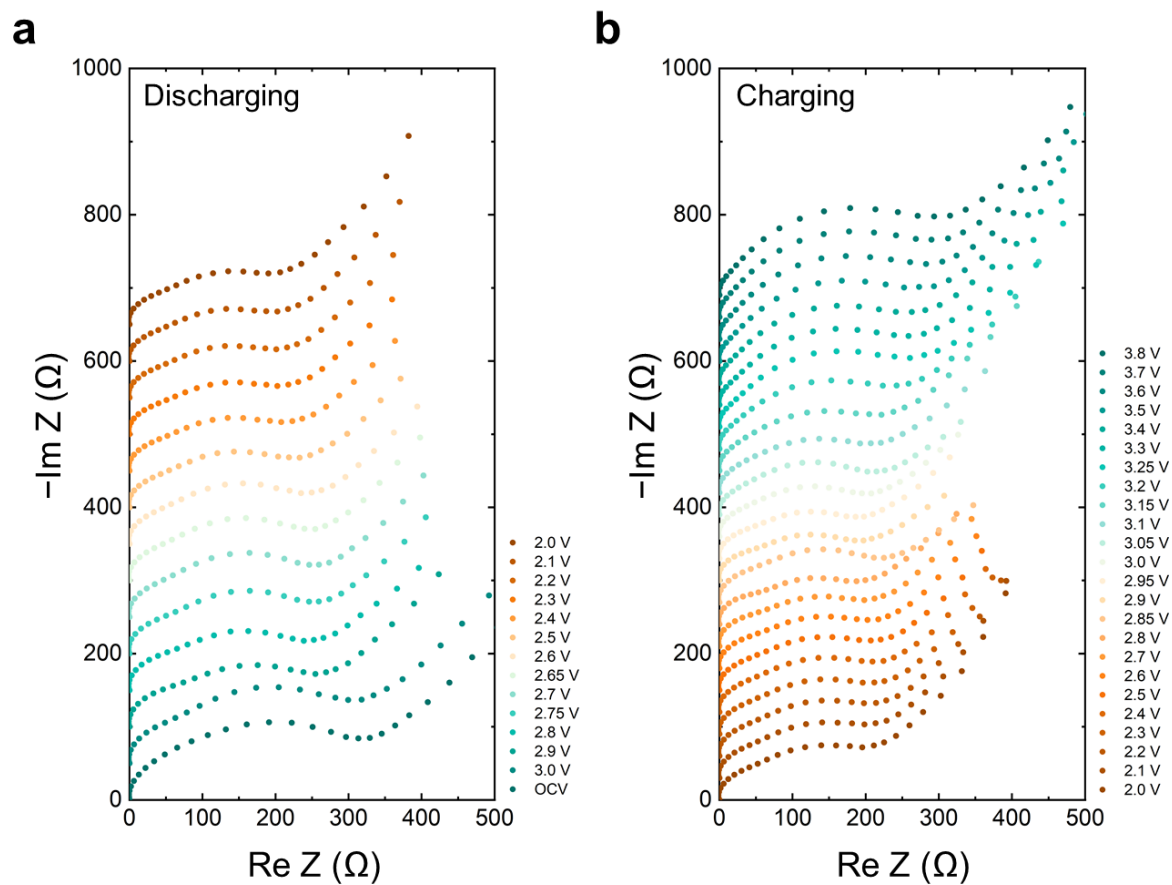


Fig. S8 *In situ* EIS results of the RO-FP electrode at 25 °C (a) obtained after constant voltage discharging from open circuit voltage (OCV) to 2.0 V, and (b) obtained after constant voltage charging from 2.0 V to 3.8 V.

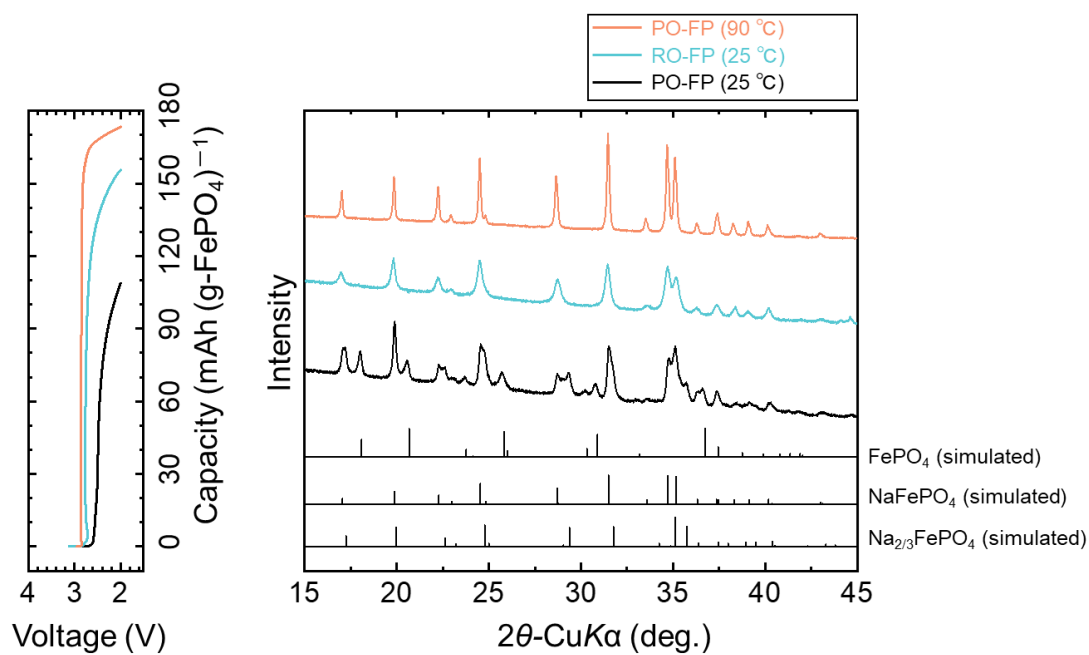


Fig. S9 *Ex situ* XRD patterns of the FePO₄ electrodes after the first discharge. Rate: 10 mA (g-FePO₄)⁻¹. The simulated patterns of FePO₄, NaFePO₄, and Na_{2/3}FePO₄ are calculated using VESTA software based on crystallographic data in previous reports^{1,6}.

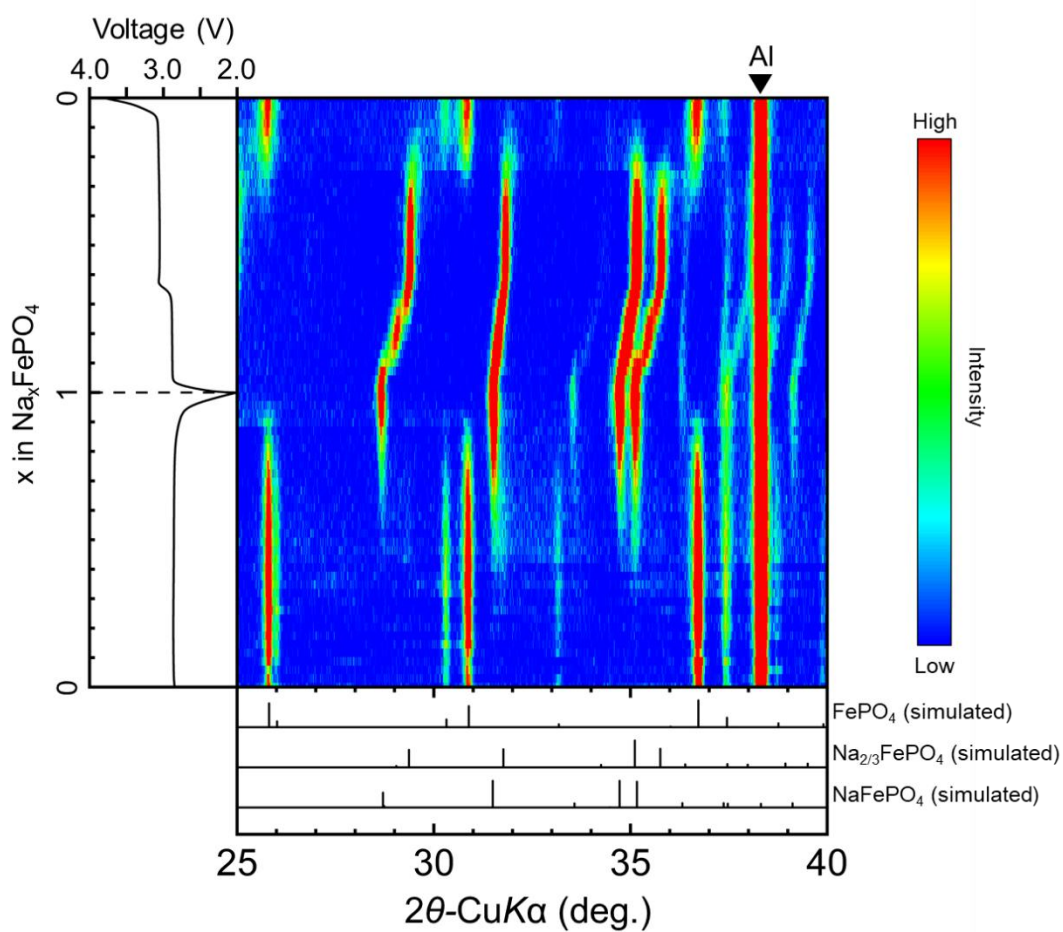


Fig. S10 *In situ* XRD of the PO-FP electrode during charge–discharge at 90 °C. Rate: 10 mA $(\text{g-FePO}_4)^{-1}$. The simulated patterns of FePO_4 , NaFePO_4 , and $\text{Na}_{2/3}\text{FePO}_4$ are calculated using VESTA software based on crystallographic data in previous reports^{1, 6}. The peak at 38.47° is assigned to Al current collector⁷.

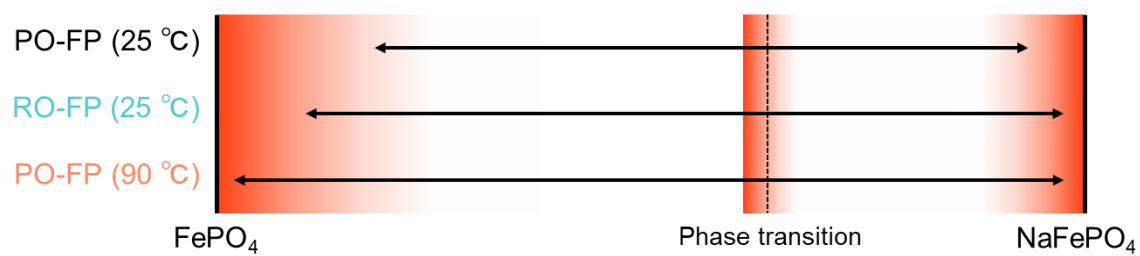


Fig. S11 An illustration of kinetic barriers for PO-FP (25 °C), RO-FP (25 °C), and PO-FP (90 °C) during charge–discharge. Darker red shading indicates higher kinetic barriers. Black arrows show the range within which the reversible sodium insertion/extraction reaction can occur.

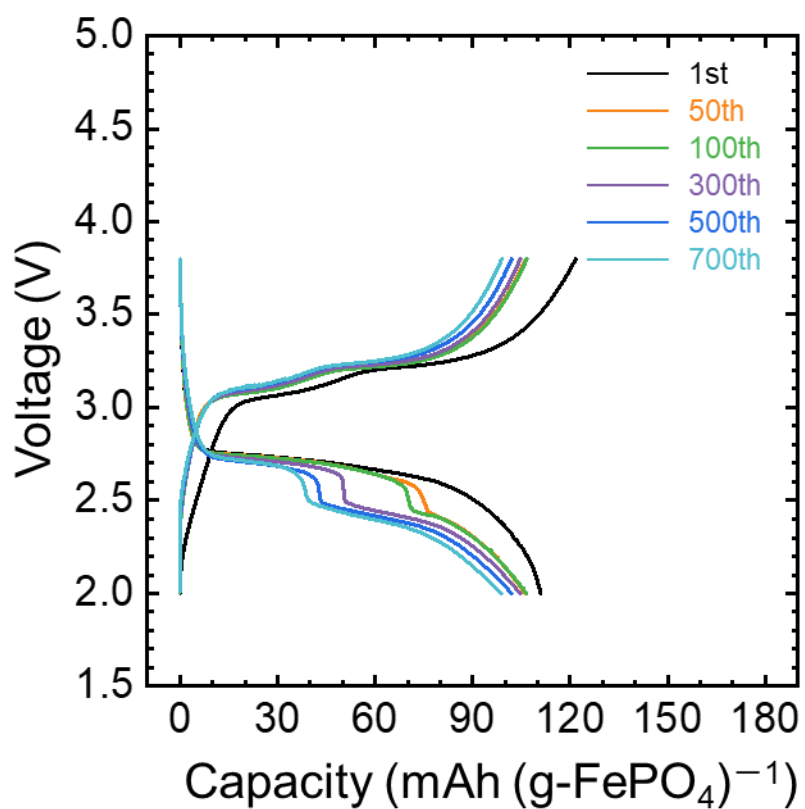


Fig. S12 Charge–discharge curves during cycle performance test of the Na/RO-FP full cell shown in **Fig. 6b** at 25 °C (N/P = 1.44). Rate: 100 mA (g-FePO₄)⁻¹.

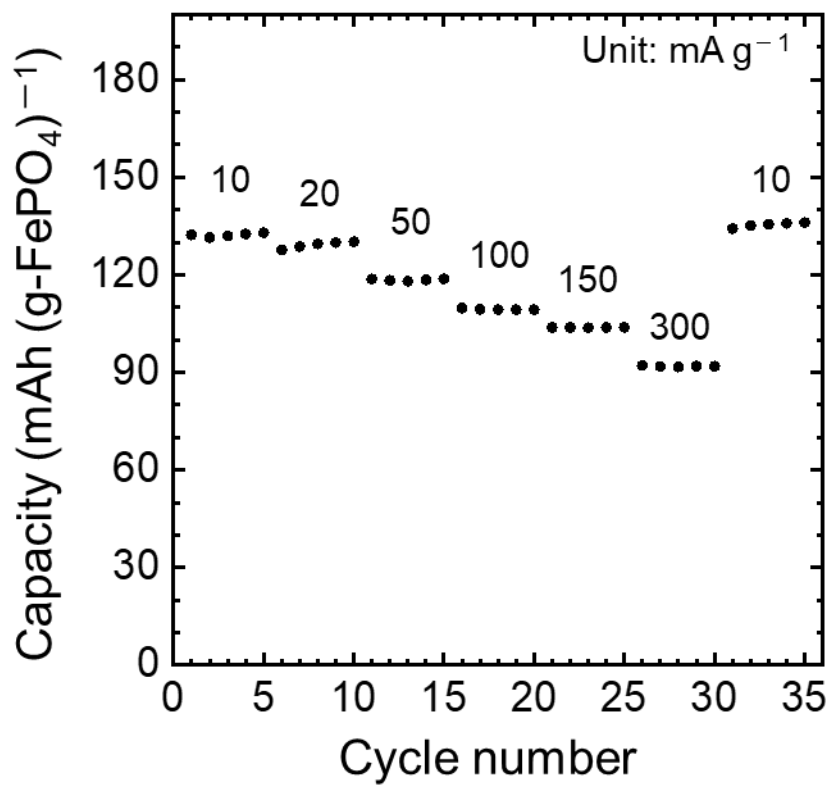


Fig. S13 Rate capability of the Na/RO-FP cell with 1 mol dm⁻³ Na[PF₆]-DME at 25 °C.

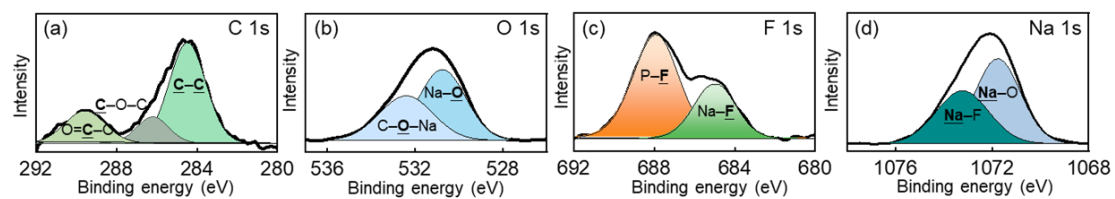


Fig. S14 XPS spectra of (a) C 1s, (b) O 1s, (c) F 1s, and (d) Na 1s regions for characterization of the SEI layer on the metallic sodium in Na/FePO₄ cell after 100 cycles at 100 mA (g-FePO₄)⁻¹. Electrolyte: 1 mol dm⁻³ Na[PF₆]-DME.

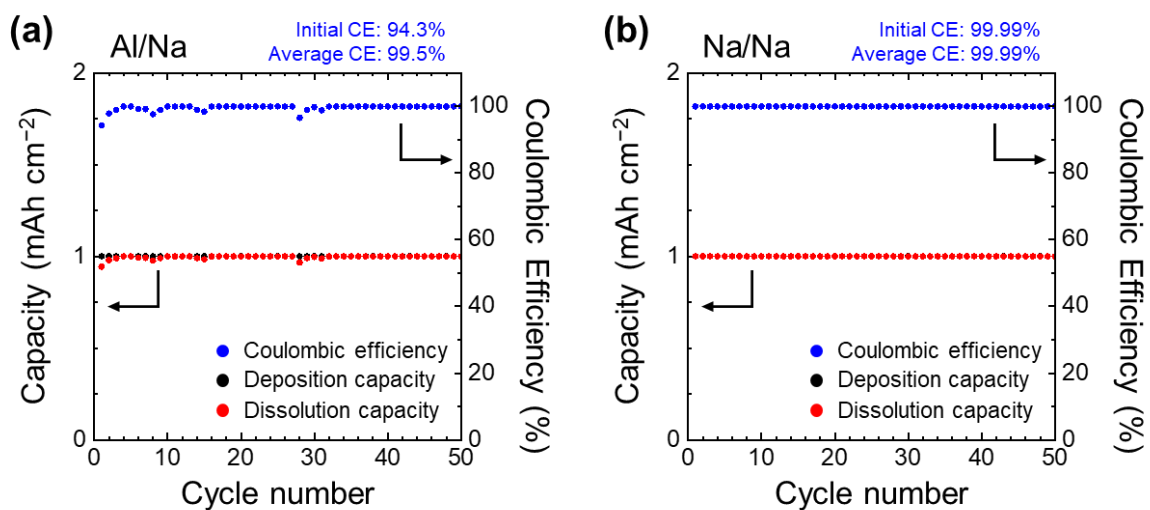


Fig. S15 Galvanostatic sodium deposition–dissolution test results of (a) Al/Na and (b) Na/Na cells at 0.5 mA cm^{-2} (1 mAh cm^{-2}). Cutoff voltage: $-1 \text{ V}-1 \text{ V}$.

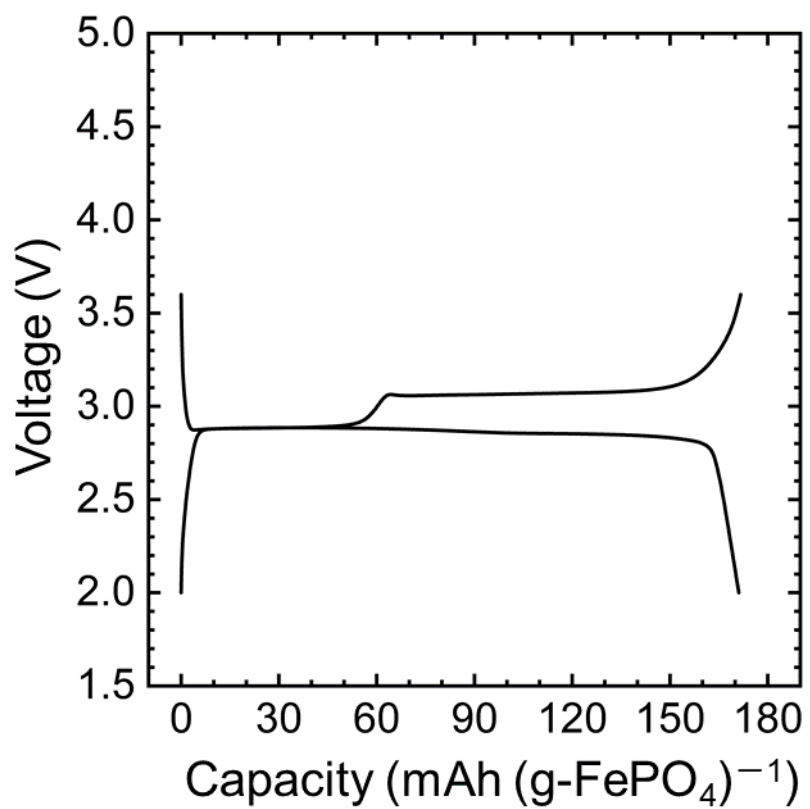


Fig. S16 Charge–discharge curves of the Na/PO-FP full cell at 90 °C (N/P = 1.20). Rate: 10 mA (g-FePO₄)⁻¹.

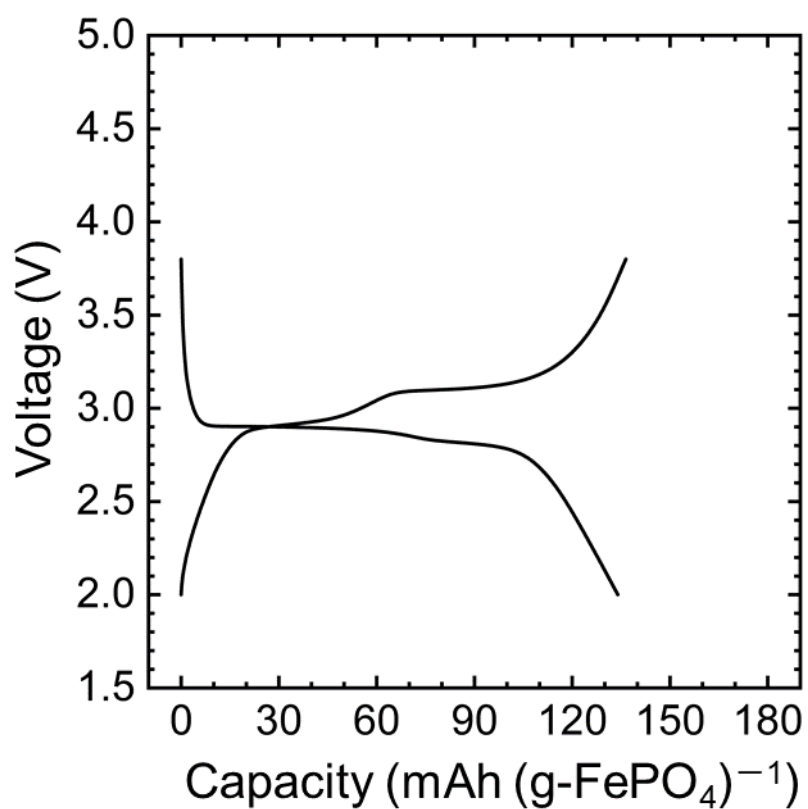


Fig. S17 Charge–discharge curves of the Na/RO-FP full cell at 25 °C (N/P = 0.56). Rate: 10 mA (g-FePO₄)⁻¹.

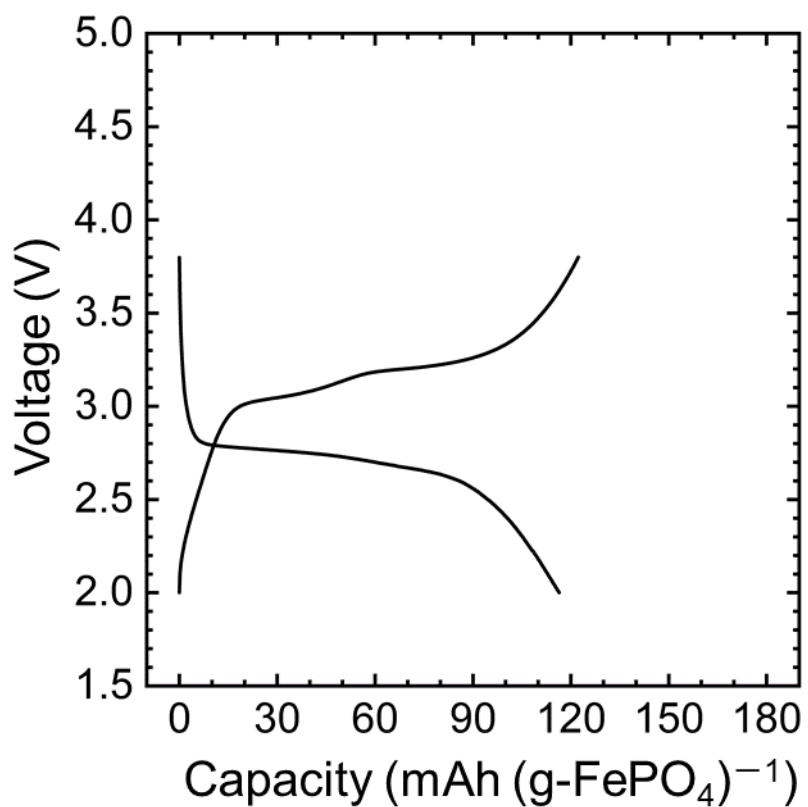


Fig. S18 Charge–discharge curves of the Na/RO-FP full cell at 25 °C (N/P = 0.56). Rate: 100 mA (g-FePO₄)⁻¹.

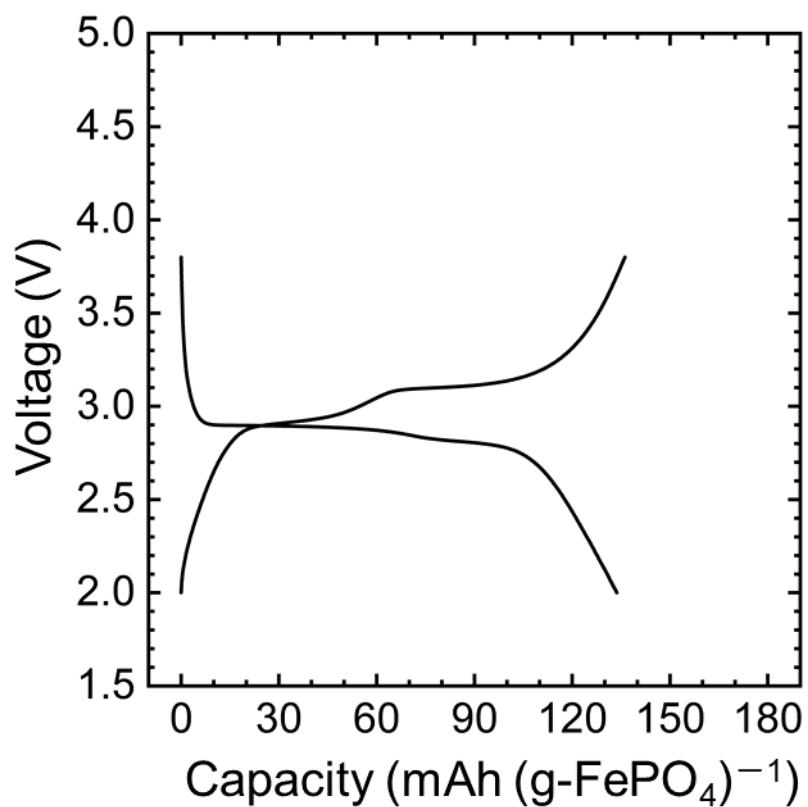


Fig. S19 Charge–discharge curves of the Na/RO-FP full cell at 25 °C (N/P = 1.44). Rate: 10 mA (g-FePO₄)⁻¹.

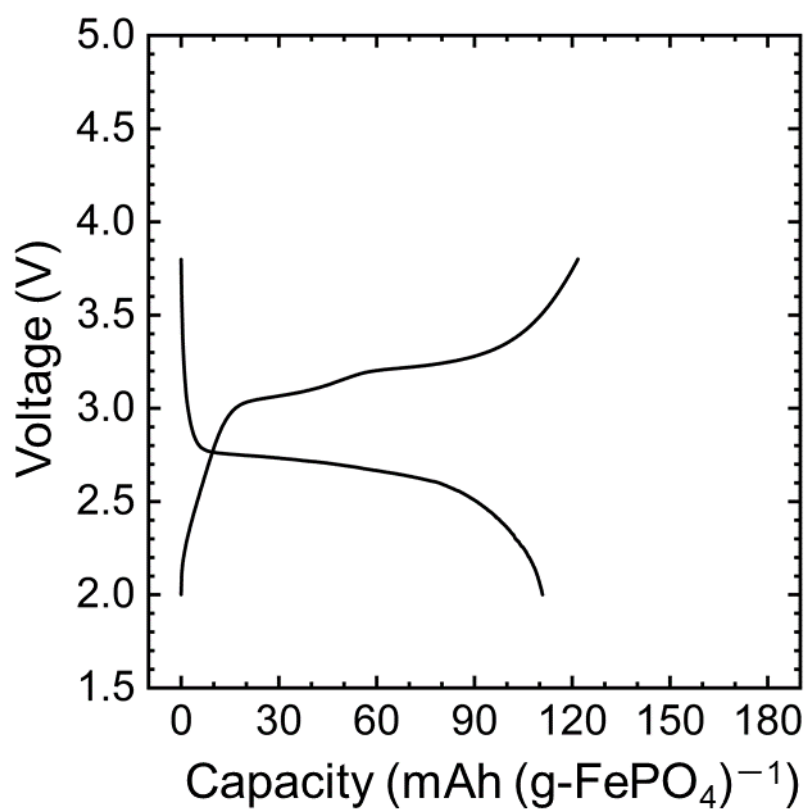


Fig. S20 Charge–discharge curves of the Na/RO-FP full cell at 25 °C (N/P = 1.44). Rate: 100 mA (g-FePO₄)⁻¹.

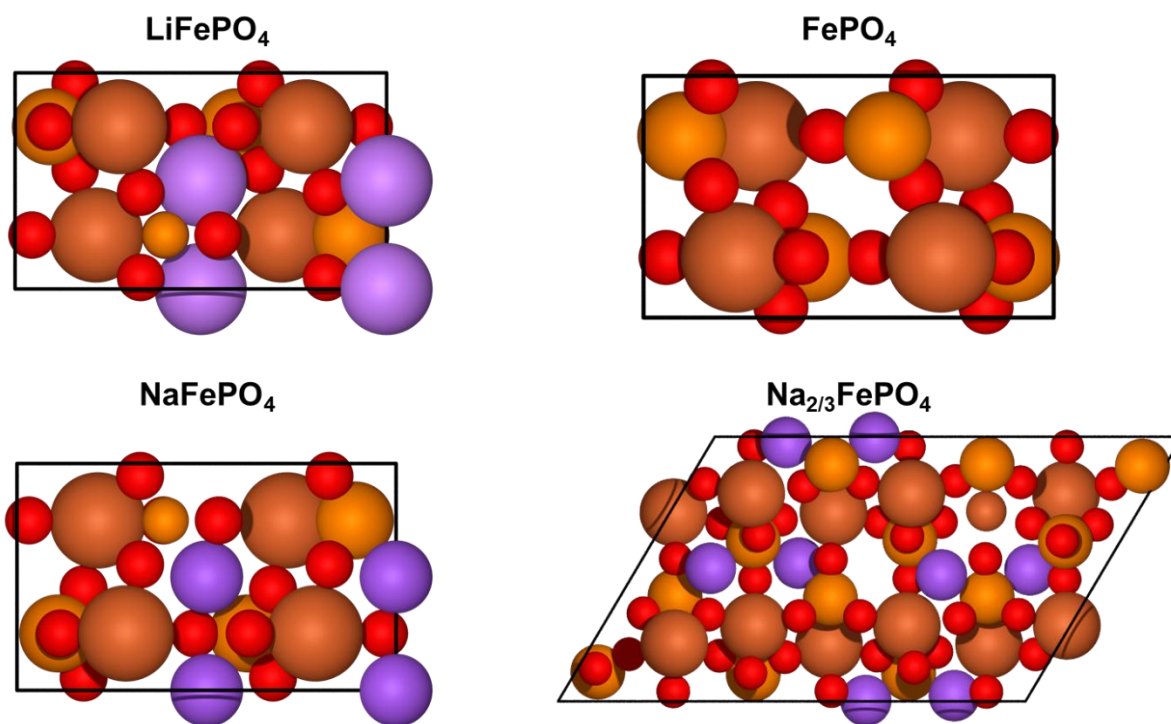


Fig. S21 Unit cell structures of NEB calculations.

References

1. A. S. Andersson, B. Kalska, L. Haggstrom and J. O. Thomas, *Solid State Ionics*, 2000, **130**, 41-52.
2. T. Li, J. Sun, S. Gao, B. Xiao, J. Cheng, Y. Zhou, X. Sun, F. Jiang, Z. Yan and S. Xiong, *Adv. Energy Mater.*, 2021, **11**, 2003699.
3. S. Wu, T. Wada, H. Shionoya, J. Hwang, K. Matsumoto and R. Hagiwara, *Energy Storage Mater.*, 2023, **61**, 102897.
4. J. Chen, Y. Peng, Y. Yin, M. Liu, Z. Fang, Y. Xie, B. Chen, Y. Cao, L. Xing, J. Huang, Y. Wang, X. Dong and Y. Xia, *Energy Environ. Sci.*, 2022, **15**, 3360-3368.
5. X. Zhang, F. Hao, Y. Cao, Y. Xie, S. Yuan, X. Dong and Y. Xia, *Adv. Funct. Mater.*, 2021, **31**, 2009778.
6. P. Moreau, D. Guyomard, J. Gaubicher and F. Boucher, *Chem. Mater.*, 2010, **22**, 4126-4128.
7. H. E. Swanson and E. Tatge, in *Standard X-ray Diffraction Powder Patterns*, National Bureau of Standards, 1953, vol. 1, ch. 2.2, pp. 11-12.